Validation of Formation Keeping Control for GPS-based Satellite Formation Flying

Jae-Ik Park [(1)], **Han-Earl Park** [(2)], **and Moon-Beom Heo** [(3)]
[(1)(3)]*Korea Aerospace Research Institute,*
Daejeon 305-333, Republic of Korea, (+82)42-870-3976, jpark@kari.re.kr
[(2)]*Yonsei University,*
Seoul 120-749, Republic of Korea, (+82)2-2123-2577, hanearl@yonsei.ac.kr

Abstract: *This research is to validate state-dependent Riccati equation (SDRE) control performance using a GPS based hardware-in-the-loop (HIL) testbed. The SDRE nonlinear control technique with the new developed state-dependent coefficient (SDC) form is applied to the formation-keeping. The established SDC form can be formulated to include all the nonlinearities in the relative dynamics and J2 orbital perturbation. To validate the SDRE formation keeping control developed, a closed-loop HIL testbed was configured, and a test formation flying scenario was established. The developed formation-keeping controller has robustness in a variety of perturbations, such as the gravity perturbation, air drag and solar pressure etc.*

Keywords: *GPS, Satellite Formation-Flying, Formation Keeping, Control, Validation*

1. Introduction

Satellite formation flying is an attractive alternative to the traditional single satellite mission architecture. This is because in using several small satellites, space missions can be more efficient, flexible, and cost effective. Many innovative formation flying missions, such as virtual telescopes for astronomical observations, laser interferometers for the detection of gravitational waves, and synthetic aperture radar interferometers have been proposed in the last few decades. The gravity recovery and climate experiment (GRACE) mission, for example, uses a pair of satellites flying in formation in a low earth orbit (LEO) to make accurate gravitational measurements. The TerraSAR-X add-on for Digital Elevation Measurements (TanDEM-X) mission will fly in close formation with the already launched TerraSAR-X satellite to provide elevation measurements of the Earth's surface. TerraSAR-X is one of the several missions proposed that will use formation flying satellites for synthetic aperture radar (SAR). The PRISMA mission is a Swedish micro-satellite mission aimed at the demonstration and flight validation of key technologies for formation flying [1].

The most challenging aspects of satellite formation flying missions are the relative navigation and control of satellites in formation flying. In particular, relative navigation plays a key role in formation flying. The global positioning system (GPS) can be an important component of navigation sensors because it provides measurement data processed for determining the precise state. Satellite formation flying also involves controlling the relative position between satellites. The primary concern with satellite formation flying is fuel consumption. Controller design is crucial for the purpose of conserving fuel, and a good satellite controller is one that will use as little fuel as possible to accomplish the maneuver. Control strategies for formation flying control in

the presence of several perturbations have been conducted by various researchers. Kong [2] has discussed the optimal cluster trajectories for the reconfiguration problem, which has been applied to solve minimum energy problems using Hill's equation and a linearized J2 model. Kim et al. [3] has developed a multi-impulse guidance scheme in Hill's frame for satellites flying in formation on the basis of a set of relative orbital elements, including the first-order effects of J2 perturbations. Sparks [4] has studied the performance of linear quadratic regulators (LQR) for satellite formation keeping in the presence of gravity perturbations. Schaub and Alfriend [5] discussed the effects of applying impulsive control on orbital elements that were perturbed by the J2 effect. The control laws for formation establishment and keeping have also been presented by Vadali and Vaddi [6]. Vaddi and Vadali [7] presented Lyapunov, LQR, and period-matching control schemes that generate circular projected orbits. All of these studies, however, consider the linear control technique or linearized relative dynamics. Gurfil et al. [8] presented a novel nonlinear adaptive neural control methodology for the challenging problem of deep-space spacecraft formation flying. Some previous studies have applied the state-dependent Riccati equation (SDRE) nonlinear control technique to satellite formation flying. Irvin and Jacques [9] compared various linear and nonlinear control techniques such as LQR, LQR with linearizing feedback, SDRE, and sliding mode control. However, the orbit of the chief satellite was assumed to be circular, and the state-dependent coefficient (SDC) form that was designed included a singularity. The chief satellite's circular orbit may cause a large position error in the case of elliptic orbits, and the singularity can make the system unstable. Won and Ahn [10] also applied the SDRE control technique to non-coplanar formation flying with a constant separation distance, and to in-plane formation flying with a large angle of separation; they extended the chief orbit to an elliptical orbit. Nevertheless, some nonlinearities of relative motion were ignored in this study when the SDC form was designed, and this caused a rather large position error and reconfiguration problems. Park et al. [11] established that an SDC form can be formulated to include all the nonlinearities in the relative dynamics and J2 orbital perturbation.

However, it is a challenge to validate the SDRE formation keeping control in the relative dynamic system with perturbation. Hence, the final objective of this research is to validate SDRE control performance using a GPS-based hardware-in-the-loop (HIL) simulation testbed. The SDRE technique is utilized as a nonlinear controller for the satellite formation keeping problem. For the SDRE controller, SDC form is formulated to include nonlinearities in the relative dynamics and J_2 orbital perturbation. Finally, to validate the formation keeping controller developed, a closed-loop HIL simulation testbed was configured and a test formation flying scenario was established [12]. The current paper consists of four three sections and conclusions. In Section 2, the SDRE technique is briefly introduced to establish the SDRE controller with the SDC form for the nonlinear relative dynamics and the SDC forms are formulated from general nonlinear equations of relative motions. Section 3 presents discussions on the HIL simulation settings for closed-loop HIL simulation. Simulation results for closed-loop formation keeping are also presented. Finally, conclusions are given in Section 4.

2. SDRE Technique for Satellite Formation Keeping Control

By using the SDRE control technique, which was introduced by Cloutier [13], a nonlinear dynamic equation can be reformulated into an SDC form and a Riccati equation can be solved for the LQR control technique. The SDRE control technique is intuitively similar to the LQR technique in terms of the tradeoff between the control effort and state errors. Furthermore, the SDRE control technique has good robustness properties, similar to the LQR. Since the SDRE control law varies through the state of satellite, it allows more accurate control of nonlinearity as the distance between two satellites and orbital eccentricity change. Thus, a nonlinear control technique of the SDRE is utilized to solve the formation keeping control problem based on the SDC form developed.

2.1 State-Dependent Riccati Equation

The SDRE control technique is used to control the relative nonlinear system. A general nonlinear dynamic system is given by

$$\dot{\vec{x}} = \vec{f}(\vec{x}) + g(\vec{x})\vec{u} \tag{1}$$

where $\vec{x} \in R^n$, $\vec{u} \in R^m$. It is assumed that $\vec{f}(0) = \vec{0}$ and $g(\vec{x}) \neq 0$ for all $\vec{x}$. The optimization problem is to find the control, $\vec{u}$, that minimizes the performance index

$$J = \frac{1}{2}\int_{t_0}^{t_f} \left(\vec{x}^T Q(\vec{x})\vec{x} + \vec{u}^T R(\vec{x})\vec{u}\right) dt \tag{2}$$

where Q is a real symmetric positive semi-definite matrix, and R is a real symmetric positive definite matrix. The SDRE obtains a suboptimal solution to the above problem. Using direct parameterization of $\vec{f}(\vec{x}) = A(\vec{x})\vec{x}$ and $g(\vec{x}) = B(\vec{x})$, the nonlinear Equation of relative motion can be transformed to a SDC form

$$\dot{\vec{x}} = A(\vec{x})\vec{x} + B(\vec{x})\vec{u} \tag{3}$$

Note that the choice of $A(\vec{x})$ is not unique, and this may lead to a suboptimal controller. The SDRE controller solves the state-dependent Riccati equation to obtain $K(\vec{x}) \geq 0$

$$K(\vec{x})A(\vec{x}) + A^T(\vec{x})K(\vec{x}) - K(\vec{x})B(\vec{x})R^{-1}(\vec{x})B^T(\vec{x})K(\vec{x}) + Q(\vec{x}) = 0 \tag{4}$$

Then, the SDRE controller uses the nonlinear control law

$$\vec{u}(\vec{x}) = -R^{-1}(\vec{x})B^T(\vec{x})K(\vec{x})\vec{x} \tag{5}$$

Note that the Riccati matrix, $K(\vec{x})$, depends on the choice of $A(\vec{x})$. Because $A(\vec{x})$ is not unique, there are multiple suboptimal solutions. In addition, Cloutier [13] proves that if

$A(\vec{x})$, $B(\vec{x})$, $Q(\vec{x})$, and $R(\vec{x})$ are smooth, and the pair $[A(\vec{x}), B(\vec{x})]$ is point-wise stabilize, for all $\vec{x}$, then the SDRE produces a closed-loop solution which is locally asymptotically stable.

2.2. Nonlinear Equation of Relative Motion

A general nonlinear equation of relative motion is expressed as

$$\begin{pmatrix} \ddot{x} - 2\dot{\nu}\dot{y} - \ddot{\nu}y - \dot{\nu}^2 x + \frac{\mu}{\gamma}x + \frac{\mu}{\gamma}r_c - \frac{\mu}{r_c^2} \\ \ddot{y} + 2\dot{\nu}\dot{x} + \ddot{\nu}x - \dot{\nu}^2 y + \frac{\mu}{\gamma}y \\ \ddot{z} + \frac{\mu}{\gamma}z \end{pmatrix} = \begin{pmatrix} a_x \\ a_y \\ a_z \end{pmatrix} \tag{6}$$

where x, y and z are state variables to describe the relative position vector, $\vec{\rho}$, in the $\hat{e}_x$, $\hat{e}_y$ and $\hat{e}_z$ axes, respectively, and a_x, a_y and a_z are the orbital perturbation terms, such as the geopotential, thrust, air drag, and solar radiation pressure. ν is the true anomaly of the chief, r_c is the radius of the chief orbit and μ is a gravitational parameter. Finally, γ is defined as

$$\gamma \equiv \left|\vec{r}_c + \vec{\rho}\right|^3 = \left((r_c + x)^2 + y^2 + z^2\right)^{3/2} \tag{7}$$

Equation 6 is equal to Hill's equation when the chief orbit is a circular orbit and the distance between the chief and deputy is very close.

2.3. State-Dependent Coefficient (SDC) Form with J2 Orbital Perturbation

We rewrite the term of $\left(\frac{\mu}{\gamma}r_c - \frac{\mu}{r_c^2}\right)$ in Eq. 6 to preserve the non-linearity as much as possible and to avoid a singularity. Using Eq. 7, the term can be expressed in the following form

$$\frac{\mu}{\gamma}r_c - \frac{\mu}{r_c^2} = \mu\left(\frac{r_c}{\left(1 + \frac{2}{r_c}x + \frac{x^2 + y^2 + z^2}{r_c^2}\right)^{3/2}}\frac{1}{r_c^3} - \frac{1}{r_c^2}\right) \tag{8}$$

Let's define

$$\xi \equiv -\frac{2}{r_c}x - \frac{x^2 + y^2 + z^2}{r_c^2} = \left(-\frac{2}{r_c} - \frac{x}{r_c^2}\right)x + \left(-\frac{y}{r_c^2}\right)y + \left(-\frac{z}{r_c^2}\right)z \tag{9}$$

Then, by negative binomial series 0, Equation 9 becomes

$$\frac{\mu}{\gamma}r_c-\frac{\mu}{r_c^2}=\frac{\mu}{r_c^2}\left(\left(1-\xi\right)^{-\frac{3}{2}}-1\right)=\frac{3}{2}\frac{\mu}{r_c^2}\Psi\xi \tag{10}$$

where Ψ is defined as a series

$$\Psi\equiv 1+\psi_1+\psi_2+\cdots,\ \psi_1\equiv\frac{\left(\frac{3}{2}+1\right)}{2}\xi,\ \psi_2\equiv\frac{\left(\frac{3}{2}+2\right)}{3}\psi_1\xi,\ \psi_3\equiv\frac{\left(\frac{3}{2}+3\right)}{4}\psi_2\xi,\cdots \tag{11}$$

Consequently, Equation 6 becomes

$$\begin{pmatrix}\dot{x}_1\\ \dot{x}_2\\ \dot{x}_3\\ \dot{x}_4\\ \dot{x}_5\\ \dot{x}_6\end{pmatrix}=\begin{bmatrix}0 & 1 & 0 & 0 & 0 & 0\\ \dot{\nu}^2-\frac{\mu}{\gamma}+\frac{3}{2}\frac{\mu}{r_c^3}\left(2+\frac{x}{r_c}\right)\Psi & 0 & \ddot{\nu}+\frac{3}{2}\frac{\mu}{r_c^4}y\Psi & 2\dot{\nu} & \frac{3}{2}\frac{\mu}{r_c^4}z\Psi & 0\\ 0 & 0 & 0 & 1 & 0 & 0\\ -\ddot{\nu} & -2\dot{\nu} & \dot{\nu}^2-\frac{\mu}{\gamma} & 0 & 0 & 0\\ 0 & 0 & 0 & 0 & 0 & 1\\ 0 & 0 & 0 & 0 & -\frac{\mu}{\gamma} & 0\end{bmatrix}\begin{pmatrix}x_1\\ x_2\\ x_3\\ x_4\\ x_5\\ x_6\end{pmatrix}+\begin{bmatrix}0 & 0 & 0\\ 1 & 0 & 0\\ 0 & 0 & 0\\ 0 & 1 & 0\\ 0 & 0 & 0\\ 0 & 0 & 1\end{bmatrix}\begin{pmatrix}u_1\\ u_2\\ u_3\end{pmatrix} \tag{12}$$

where state variables, x_1, x_2, x_3, x_4, x_5 and x_6 are x, $\dot{x}$, y, $\dot{y}$, z and $\dot{z}$ in the LVLH coordinate, respectively. Equation 12 has the structure described in Eq. 3, and is the newly developed SDC form without J_2 perturbation

In the LVLH coordinate system, the acceleration ($\vec{a}_{J_2}$) of J2 perturbation is expressed as

$$\vec{a}_{J_2}=-\frac{3\mu R_e^2 J_2}{r^4}\left[\left(\frac{1}{2}-\frac{3\sin^2 i\sin^2\theta}{2}\right)\hat{e}_x+\sin^2 i\sin\theta\cos\theta\,\hat{e}_y+\sin i\sin\theta\cos i\,\hat{e}_z\right] \tag{13}$$

where R_e is the mean radius of the Earth, r is the radius from the center of the Earth, J2 is the coefficient of J2 perturbation, i is the inclination. Then, the equation of motion with J2 perturbation for the chief satellite and the deputy satellite are

$$\begin{aligned}\ddot{\vec{r}}_c&=\vec{g}(\vec{r}_c)+\vec{a}_{J_2}(\vec{r}_c)\\ \ddot{\vec{r}}_d&=\vec{g}(\vec{r}_d)+\vec{a}_{J_2}(\vec{r}_d)\end{aligned} \tag{14}$$

Then Eq. 13 becomes

$$\vec{a}_{J_2}=-\frac{3}{2}\frac{J_2\mu R_e^2}{r^4}\left[J_x(i,\theta)\hat{e}_x+J_y(i,\theta)\hat{e}_y+J_z(i,\theta)\hat{e}_z\right] \tag{15}$$

where the argument of latitude is $\theta \equiv \omega + \nu$, J index is defined as follows

$$\begin{aligned} J_x(i,\theta) &\equiv 1 - 3\sin^2 i \sin^2\theta \\ J_y(i,\theta) &\equiv 2\sin^2 i \sin\theta\cos\theta = \sin^2 i \sin 2\theta \\ J_z(i,\theta) &\equiv 2\sin i \cos i \sin\theta = \sin 2i \sin\theta \end{aligned} \tag{16}$$

Substituting Eq. 13 with Eq. 14 yields

$$\begin{aligned} \ddot{\vec{r}}_c + \ddot{\vec{\rho}} = &-\frac{\mu}{\left|\vec{r}_c + \vec{\rho}\right|^3}\left(\vec{r}_c + \vec{\rho}\right) \\ &-\frac{3}{2}\frac{J_2 \mu R_e^2}{\left|\vec{r}_c + \vec{\rho}\right|^4}\left[J_x(i_d,\theta_d)\hat{e}_x + J_y(i_d,\theta_d)\hat{e}_y + J_z(i_d,\theta_d)\hat{e}_z\right] \end{aligned} \tag{17}$$

where $\ddot{\vec{r}}_c = -\frac{\mu}{\left|\vec{r}_c\right|^3}\vec{r}_c - \frac{3}{2}\frac{J_2\mu R_e^2}{\left|\vec{r}_c\right|^4}\left[J_x(i_c,\theta_c)\hat{e}_x + J_y(i_c,\theta_c)\hat{e}_y + J_z(i_c,\theta_c)\hat{e}_z\right]$ and Equation 17 becomes

$$\begin{aligned} &{}^s\ddot{\vec{\rho}} + 2\vec{\omega}\times {}^s\dot{\vec{\rho}} + \dot{\vec{\omega}}\times {}^s\vec{\rho} + \vec{\omega}\times\left(\vec{\omega}\times {}^s\vec{\rho}\right) + \frac{\mu}{\left|\vec{r}_c + {}^s\vec{\rho}\right|^3}\left(\vec{r}_c + {}^s\vec{\rho}\right) \\ &+\frac{3}{2}\frac{J_2\mu R_e^2}{\left|\vec{r}_c + {}^s\vec{\rho}\right|^4}\begin{bmatrix} J_x(i_d,\theta_d) \\ J_y(i_d,\theta_d) \\ J_z(i_d,\theta_d) \end{bmatrix} - \frac{\mu}{\left|\vec{r}_c\right|^3}\vec{r}_c - \frac{3}{2}\frac{J_2\mu R_e^2}{\left|\vec{r}_c\right|^4}\begin{bmatrix} J_x(i_c,\theta_c) \\ J_y(i_c,\theta_c) \\ J_z(i_c,\theta_c) \end{bmatrix} = \vec{a} \end{aligned} \tag{18}$$

Because the chief satellite rounds the Earth, the reference [10] relationship holds. where the superscript '*s*' notes the value in the rotating coordinate and $\vec{\omega}$ is the angular velocity of the rotating coordinate with respect to the inertial coordinate, and $\vec{\omega}$ is expressed in the rotating coordinate.

In the right side of Eq. 18, we can add other perturbation terms $\vec{a}$ due to thrust, air drag etc., if necessary. Rearranging the Eq. 18, then

$$\begin{pmatrix} \ddot{x} - 2\dot{\nu}\dot{y} - \ddot{\nu}y - \dot{\nu}^2 x + \frac{\mu}{\gamma}x + \frac{\mu}{\gamma}r_c - \frac{\mu}{r_c^2} \\ \ddot{y} + 2\dot{\nu}\dot{x} + \ddot{\nu}x - \dot{\nu}^2 y + \frac{\mu}{\gamma}y \\ \ddot{z} + \frac{\mu}{\gamma}z \end{pmatrix} - \frac{3}{2}J_2\mu R_e^2\left\{\frac{1}{r_c^4}\begin{bmatrix} J_x(i_c,\theta_c) \\ J_y(i_c,\theta_c) \\ J_z(i_c,\theta_c) \end{bmatrix} - \frac{1}{\left|\vec{r}_c + \vec{\rho}\right|^4}\begin{bmatrix} J_x(i_d,\theta_d) \\ J_y(i_d,\theta_d) \\ J_z(i_d,\theta_d) \end{bmatrix}\right\} = \begin{pmatrix} a_x \\ a_y \\ a_z \end{pmatrix} \tag{19}$$

Equation 19 has to be transferred to a SDC form in Eq. 3. To do that, the orbital elements (i, θ) need to be expressed by the state variables ($x, \dot{x}, y, \dot{y}, z, \dot{z}$).

The transformation matrix introduced by Gim and Alfriend [15] is used to convert the orbital elements into the state variables of the relative motion under J2 perturbation. Rewriting the J2 term Eq. 19 gives

$$\begin{aligned}
&\frac{3}{2}J_2\mu R_e^2\left\{\frac{1}{r_c^4}\begin{bmatrix}J_x(i_c,\theta_c)\\ J_y(i_c,\theta_c)\\ J_z(i_c,\theta_c)\end{bmatrix}-\frac{1}{\left|\vec{r}_c+\vec{\rho}\right|^4}\begin{bmatrix}J_x(i_d,\theta_d)\\ J_y(i_d,\theta_d)\\ J_z(i_d,\theta_d)\end{bmatrix}\right\}\\
&=\frac{3}{2}\frac{J_2\mu R_e^2}{r_c^4}\left(\begin{bmatrix}J_x(i_c+\delta i,\theta_c+\delta\theta)\\ J_y(i_c+\delta i,\theta_c+\delta\theta)\\ J_z(i_c+\delta i,\theta_c+\delta\theta)\end{bmatrix}-\begin{bmatrix}J_x(i_c,\theta_c)\\ J_y(i_c,\theta_c)\\ J_z(i_c,\theta_c)\end{bmatrix}\right)+\frac{3J_2\mu R_e^2}{r_c^4}\Psi'\xi\left(\begin{bmatrix}J_x(i_c+\delta i,\theta_c+\delta\theta)\\ J_y(i_c+\delta i,\theta_c+\delta\theta)\\ J_z(i_c+\delta i,\theta_c+\delta\theta)\end{bmatrix}\right)\xi
\end{aligned} \tag{20}$$

where $i_d=i_c+\delta i$, $\theta_d=\theta_c+\delta\theta$ and Ψ' is defined as

$$\Psi'\equiv 1+\psi_1'+\psi_2'+\ldots,\ \psi_1'\equiv\frac{(2+1)}{2}\xi,\ \psi_2'\equiv\frac{(2+2)}{3}\psi_1'\xi,\ \psi_3'\equiv\frac{(2+3)}{4}\psi_2'\xi,\ \cdots \tag{21}$$

The final term on the right side of Eq. 20 can be transferred into a SDC form because ξ is explicitly expressed by x, y, z in Eq. 9. Substituting Eq. 16 with the first term on the right side of Eq. 20 yields

$$\begin{aligned}
J_x(i_c+\delta i,\theta_c+\delta\theta)-J_x(i_c,\theta_c)&=-3\sin^2(i_c+\delta i)\sin^2(\theta_c+\delta\theta)+3\sin^2 i_c\sin^2\theta_c\\
J_y(i_c+\delta i,\theta_c+\delta\theta)-J_y(i_c,\theta_c)&=\sin^2(i_c+\delta i)\sin\left[2(\theta_c+\delta\theta)\right]-\sin^2 i_c\sin 2\theta_c\\
J_z(i_c+\delta i,\theta_c+\delta\theta)-J_z(i_c,\theta_c)&=\sin\left[2(i_c+\delta i)\right]\sin(\theta_c+\delta\theta)-\sin 2i_c\sin\theta_c
\end{aligned} \tag{22}$$

Rewriting Eq. 22 using the Taylor series, then, gives

$$\begin{aligned}
&-3\sin^2(i+\delta i)\sin^2(\theta+\delta\theta)+3\sin^2 i\sin^2\theta\\
&=-3\left[(i+\delta i)^2(\alpha_i+\beta_i)^2(\theta+\delta\theta)^2(\alpha_\theta+\beta_\theta)^2-i^2\alpha_i^2\theta^2\alpha_\theta^2\right]\\
&\sin^2(i+\delta i)\sin\left[2(\theta+\delta\theta)\right]-\sin^2 i\sin 2\theta\\
&=\left(i^2\alpha_i^2 2\theta\right)\eta_{2\theta}2\delta\theta+i^2\alpha_i^2\left(\alpha_{2\theta}+\beta_{2\theta}\right)2\delta\theta+i^2\left(2\theta+2\delta\theta\right)\left(\alpha_{2\theta}+\beta_{2\theta}\right)\left(2\alpha_i+\beta_i\right)\eta_i\delta i\\
&+\left(\alpha_i+\beta_i\right)^2\left(2\theta+2\delta\theta\right)\left(\alpha_{2\theta}+\beta_{2\theta}\right)\left(2i+\delta i\right)\delta i\\
&\sin\left[2(i+\delta i)\right]\sin(\theta+\delta\theta)-\sin 2i\sin\theta\\
&=2i\alpha_{2i}\theta\eta_\theta\delta\theta+2i\alpha_{2\theta}(\alpha_\theta+\beta_\theta)\delta\theta+2i(\theta+\delta\theta)(\alpha_\theta+\beta_\theta)\eta_{2i}2\delta i+(\alpha_{2i}+\beta_{2i})(\theta+\delta\theta)(\alpha_\theta+\beta_\theta)2\delta i
\end{aligned} \tag{23}$$

Equations 23 can be transferred into the SDC form. The newly developed SDC form with J2 perturbation is

$$\begin{pmatrix}\dot{x}_1\\ \dot{x}_2\\ \dot{x}_3\\ \dot{x}_4\\ \dot{x}_5\\ \dot{x}_6\end{pmatrix}=\begin{bmatrix}A_{J_2}(1,1) & A_{J_2}(1,2) & A_{J_2}(1,3) & A_{J_2}(1,4) & A_{J_2}(1,5) & A_{J_2}(1,6)\\ A_{J_2}(2,1) & A_{J_2}(2,2) & A_{J_2}(2,3) & A_{J_2}(2,4) & A_{J_2}(2,5) & A_{J_2}(2,6)\\ A_{J_2}(3,1) & A_{J_2}(3,2) & A_{J_2}(3,3) & A_{J_2}(3,4) & A_{J_2}(3,5) & A_{J_2}(3,6)\\ A_{J_2}(4,1) & A_{J_2}(4,2) & A_{J_2}(4,3) & A_{J_2}(4,4) & A_{J_2}(4,5) & A_{J_2}(4,6)\\ A_{J_2}(5,1) & A_{J_2}(5,2) & A_{J_2}(5,3) & A_{J_2}(5,4) & A_{J_2}(5,5) & A_{J_2}(5,6)\\ A_{J_2}(6,1) & A_{J_2}(6,2) & A_{J_2}(6,3) & A_{J_2}(6,4) & A_{J_2}(6,5) & A_{J_2}(6,6)\end{bmatrix}\begin{pmatrix}x_1\\ x_2\\ x_3\\ x_4\\ x_5\\ x_6\end{pmatrix}+\begin{bmatrix}0 & 0 & 0\\ 1 & 0 & 0\\ 0 & 0 & 0\\ 0 & 1 & 0\\ 0 & 0 & 0\\ 0 & 0 & 1\end{bmatrix}\begin{pmatrix}u_1\\ u_2\\ u_3\end{pmatrix} \quad (24)$$

The components of the matrix A_{J_2} are listed by Park et al. [11] in greater detail. The new SDC form with J2 perturbation is successfully established.

2.4. Formation Keeping Control using SDRE

For formation keeping, an optimization cost can be represented by the performance index

$$J_{FK}=\int_0^\infty\left((\vec{x}-\vec{x}_d)^T Q(\vec{x}-\vec{x}_d)+\vec{u}^T R\vec{u}\right)dt \quad (25)$$

where $\vec{x}_d$ is the desired states (position and velocity vectors of the deputy) that can be determined with respect to time when a desired formation geometry is set. $\vec{x}$ is the states describing the deputy's position and velocity with respect to the chief, and subscript 'FK' means Formation Keeping. Q and R are weighting matrixes determined by considering the trade-off between the required energy and formation keeping error. For formation keeping, $\vec{x}$ is forced to be $\vec{x}_d$ using the SDRE control law given as

$$\vec{u}=-R^{-1}B^T K(\vec{x})(\vec{x}-\vec{x}_d) \quad (26)$$

where K is a positive-definite solution of the algebraic matrix Riccati equation

$$K(\vec{x})A(\vec{x})+A(\vec{x})^T K(\vec{x})-K(\vec{x})BR(\vec{x})^{-1}B^T K(\vec{x})+Q=0 \quad (27)$$

In SDRE controller, $K(\vec{x})$ and $A(\vec{x})$ matrices vary through the states. Therefore, Equation 26 has to be calculated in point-wise (every time step).

3. Validation of Satellite Formation Keeping Control

Formation-keeping allows the satellite to maintain its formation geometry under various orbital perturbations. The relative dynamics of the deputy and chief satellites in any case cannot consider all the effects from all the orbital perturbations, so that feedback control for formation-keeping is always required. It is a challenge to validate the SDRE formation keeping control in the relative dynamic system with perturbation. Hence, the objective of this research is to validate SDRE control performance using a GPS-based HIL testbed. In this section, the HIL simulation testbed configuration and a simulation

setting are presented. Simulation results for closed-loop formation keeping control are also presented.

3.1 HIL Simulation Testbed Configuration

The HIL testbed consists of a GPS RF signal simulator, GPS receiver hardware, a GPS monitoring system, a flight control system, and a remote control system [12]. The GPS signal simulator is capable of simultaneously simulating all of the GPS RF signals received by user satellites. A simulated GPS signal is then sent to a GPS receiver. The GPS receivers are fed with RF signals, and produce GPS raw measurements such as pseudorange, carrier phase, Doppler data, and broadcast ephemerides data for the GPS satellites. The GPS monitoring system receives these data, and they are sent to the flight control system. The flight control system collects simultaneous raw measurements from the GPS monitoring systems and performs filtering processes for absolute and relative navigations. In addition, the flight control system performs control processes by using real-time navigation data. The control algorithm is based entirely on the relative navigation solutions provided by filter processing. Control accelerations are transmitted to a remote control system. The remote control system numerically integrates the satellites' states and adds the control acceleration. It also controls the GPS signal simulator through the provision of the current satellite states, thereby closing the loop of the HIL simulation testbed. In this simulation, the deputy satellite is actively maneuvering, while the chief satellite is passive. Since only one L1 single frequency GPS receiver was available during this study, the navigation filter reads a chief GPS observation log file and only the deputy observations are supplied by the receiver in real time.

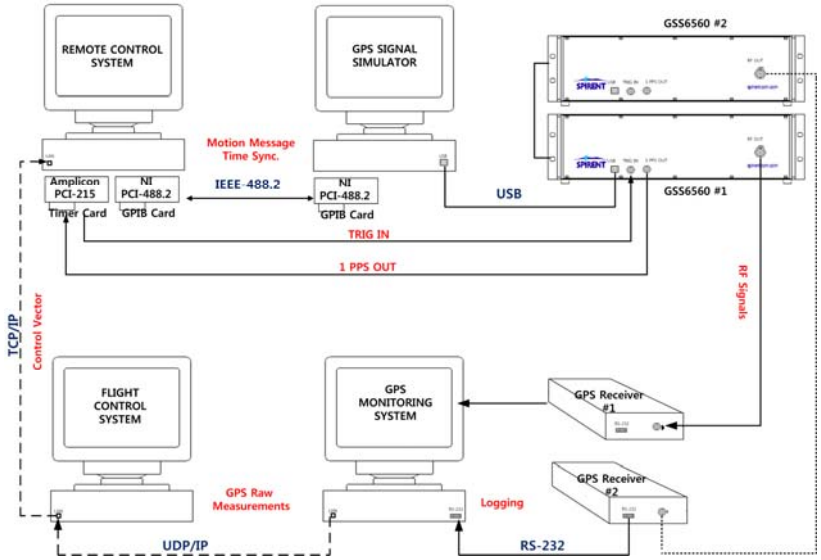

Figure 1. HIL Simulation Testbed Configuration

3.2 HIL Simulation Scenario Setup

A simulation formation flying scenario comprising a formation acquisition and keeping in a LEO has been established. The goal of the scenario is to achieve leader-follower formation flying with a 100 m along-track separation and to maintain this formation flying for some time. The initial formation flying satellite consists of two satellites in a near circular orbit with an altitude of 550 km, 97.5 degree inclination, and an initial along-track separation of 1 km.; the drag coefficient C_D is 2.3; the cross-section area for drag computation is 1 m^2; and the solar radiation pressure coefficient C_R is 1.3. For the present scenario, thrusters have been selected which can be accommodated on a small satellite and which provide small impulse bits suitable for fine formation control. A pulsed plasma thruster (PPT) system has been assumed. It provides in a doubled configuration an impulse-bit of 0.112 mN and fires at a rate of 1 Hz. The mass of the satellite is equal to 20 kg.
The initial orbital elements are listed in Tab. 1. High-fidelity satellite orbits are propagated by a precision real-time orbit propagator running on a remote control system. A numerical integration algorithm with various differential equation orders and step is applied to propagate the satellites' motion. Because the algorithm provides interpolation for a dense output, it is ideally suitable for supporting the required 100-ms period of motion messages for the GPS signal simulator. The adopted force model accounts for the Earth's gravitational field by using a 20 × 20 subset of the joint gravity model 3 (JGM-3). Furthermore, it accounts for perturbations due to atmospheric drag and solar radiation pressure, as well as solar and lunar gravitational perturbations. The Harris-Priester density model has also been adopted for atmospheric drag [16].

3.3 HIL Simulation Results

A closed-loop formation keeping simulation has been performed based on the configuration in Section 3.1. Formation keeping control is successfully achieved for the 100 m leader-follower formation flying and formation keeping begins after formation acquisition. Figure 2 shows the position difference between the deputy and chief satellites during the formation-keeping phase. Thus, the targeted leader-follower formation flying in an along-track separation of 100 m has been maintained with a mean position difference error of approximately 0.2 m and a standard deviation (1σ) of 0.9 m

Table 1. Initial Orbital Elements for Test Simulation Scenario

Orbital Elements	Chief satellite	Deputy satellite
Semi-major axis (a) [km]	6937.466	6937.466
Eccentricity (e)	0.00120	0.00120
Inclination (i) [deg]	97.615	97.615
Argument of perigee (ω) [deg]	359.951	359.951
Lon. Ascend node (Ω) [deg]	339.484	339.484
Mean anomaly (M) [deg]	0.0000450	0.0084424

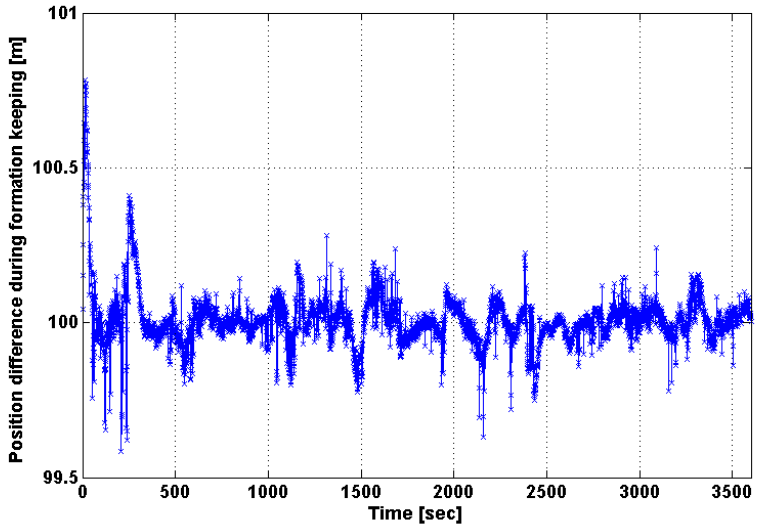

Figure 2. Position difference between the deputy and chief satellites

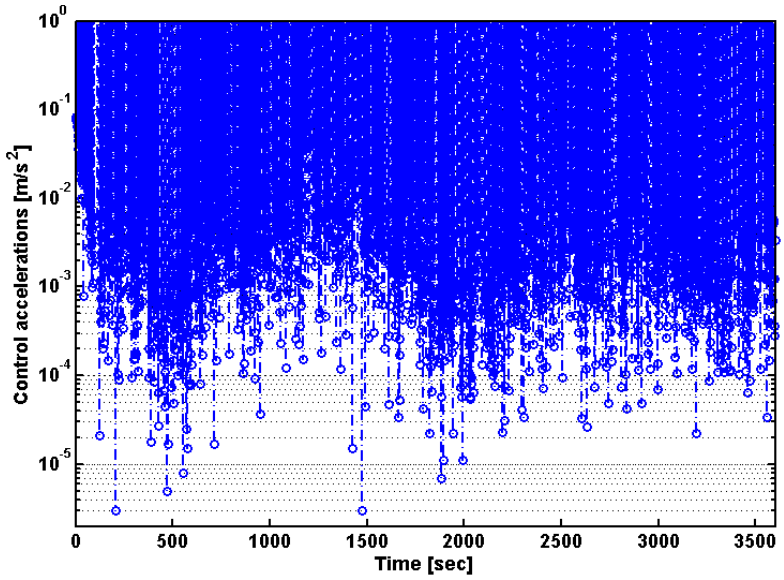

Figure 3. Control accelerations in along-track direction.

The performance of the SDRE control algorithm for formation keeping can be evaluated by the maximum, mean, and standard deviations (1σ) of the deputy satellite's state with respect to the chief satellite's state. Figure 3 shows the control accelerations in along-track direction during the formation keeping simulations. In the validation performed, a total ΔV is required of 4.8 m/s in the along-track direction to achieve formation keeping. The ΔV in the along-track direction is larger than in the other directions because the control is primarily in this direction.

4. Conclusions

In the current paper, satellite formation keeping controllers are proposed using the SDRE technique. SDC form is developed to hold all the non-linearities in the relative motion and J2 orbital perturbation to utilize the SDRE technique. The performance index of the controller is designed through tradeoff between the required energy and tracking error. To validate the SDRE formation keeping controller developed, a closed-loop HIL testbed was configured, and a test formation flying scenario was established. In the validation performed, a total ΔV is required of 4.8 m/s in the along-track direction to achieve formation keeping. The ΔV in the along-track direction is larger than in the other directions because the control is primarily in this direction. Thus, the developed SDRE controller for formation-keeping has robustness in a variety of perturbations, including the aspherical geopotential perturbation, air drag, solar radiation pressure, and third-body gravitational perturbation. The result above simulation that formation keeping controller work well during formation flying simulation.

5. Acknowledgements

This work was supported by a grant from Korea Research Council of Fundamental Science & Technology funded by Ministry of Education, Science and Technology in 2013. [Project: A Study on Satellite based Position Tracking Technology for Calamity Prevention and Public Safety Improvement]

6. References

[1] D'Amico, S., "Autonomous Formation Flying in Low Earth Orbit", Ph.D. Dissertation, Delft University of Technology, 2010.

[2] Kong, E. M. C., "Spacecraft Formation Flight Exploiting Potential Fields", Ph. D. diss., Massachusetts Institute of Technology, 2002.

[3] Kim, D.Y., Woo, B., Park, S.Y., Choi, K.H., "Hybrid optimization for multiple-impulse reconfiguration trajectories of satellite formation flying," Journal of Advances Space Research, Vol. 44, No. 11, 2009, pp. 1257–1269.

[4] Sparks, A., "Satellite Formation Keeping Control in the Presence of Gravity Perturbations," Proceedings of the American Control Conference, Chicago, Illinois, 2000, pp. 844-848.

[5] Schaub, H., Alfriend, K.T., "Impulse Feedback Control to Establish Specific Mean Orbit Elements of Spacecraft Formations," Journal of Guidance, Control, and Dynamics, Vol. 24 No. 4, 2001, pp. 739–745.

[6] Vadali, S. R. and Vaddi, S. S., “Large-Angle Kinematics for the Control of Satellite Relative Motion,” Proceedings of the AIAA/AAS Astrodynamics Conference, AAS 02-258, 2002

[7] Vaddi, S. S. and Vadali, S. R., “Linear and Nonlinear Control Laws Formation Flying”, Proceedings of the 13th AAS/AIAA Space Flight Mechanics Meeting, AAS 03-109, 2003

[8] Gurfil, P., Idan, M., Kasdin, N.J., “Adaptive Neural Control of Deep-Space Formation Flying,” Journal of Guidance, Control, and Dynamics, Vol. 26, No. 3, pp. 491-501, 2003.

[9] Irvin, D.J., Jacques, D.R., “A Study of Linear Versus Nonlinear Control Techniques for the Reconfiguration of Satellite Formations,” Advances Astronautical Science, Vol.109, 2002, pp. 589-608.

[10] Won, C.H., Ahn, H.S., “Nonlinear orbital dynamic equations and state-dependent Riccati equation control of formation flying satellites,” Journal of Astronautical Science, Vol. 51, No. 4, 2003, pp. 433-449.

[11] Park, H.E., Park, S.-Y., Choi, K.-H., “Satellite Formation Reconfiguration and Station-Keeping using State-Dependent Riccati Equation Technique,” Aerospace Science and Technology, Vol.15, 2011, pp. 440-452.

[12] Park, J.-I., Park, H.E., Park, S.-Y., Choi, K.-H., “Hardware-in-the-loop Simulations of GPS-based Navigation and Control for Satellite Formation Flying,” Advances in Space Research, Vol. 46, 2010, pp.1451-1465.

[13] Cloutier, J. R., “State-Dependent Riccati Equation Techniques: An Overview”, Proceedings of the American Control Conference, 4-6 June, at Albuquerque, New Mexico, 1997, pp. 932-933.

[14] Arfken, G. B. and Weber, H. J., “Mathematical Methods for Physicists,” 5th ed, Academic Press, 2001, pp. 338-339.

[15] Gim, D. W. and Alfriend, K. T., “State Transition Matrix of Relative Motion for the Perturbed Noncircular Reference Orbit,” Journal of Guidance, Control, and Dynamics, Vol. 26, No. 6, 2003, pp. 956-971.

[16] Montenbruck, O., Gill, E., “Satellite Orbits,” Springer-Verlag, Heidelberg, Germany, 2001.